



Photophysical and Electrochemical Studies of Anchored Chromium (III) Complex on Reduced Graphene Oxide via Diazonium Chemistry

Jemini Jose¹ | Athimotlu Raju Rajamani² | Sreekanth Anandaram³  | Sujin P. Jose⁴ | Sebastian C. Peter² | Sreeja P B¹ 

¹ Department of Chemistry, CHRIST (Deemed to be University), Bengaluru 560029, India

² New Chemistry Unit, School of Advanced Materials, Jawaharlal Nehru Centre for Advanced Scientific Research, Jakkur, Bengaluru 560064, India

³ Department of Chemistry, National Institute of Technology, Tiruchirappalli 620015, India

⁴ School of Physics, Madurai Kamaraj University, Madurai 625021, India

Correspondence

Sreeja P B, Department of Chemistry, CHRIST (Deemed to be University), Bengaluru 560029, India.
Email: sreeja.pb@christuniversity.in

Covalently anchored chromium complex on reduced graphene oxide (rGO-Cr) is successfully synthesised through trimethoxy silyl propanamine (TMSPA) and phenyl azo salicylaldehyde (PAS) coupling. The rGO-Cr is characterised by Fourier transform infrared spectroscopy (FTIR), X-ray diffraction (XRD), X-ray photoelectron spectroscopy (XPS), electron dispersive analysis of X-rays (EDAX), Raman spectroscopy, scanning electron microscopy (SEM) and high resolution transmission electron microscopy (HRTEM). Absorption and emission properties of rGO-TMSPA-PAS are studied by excitation dependent photoluminescence emissions at room temperature. Electrochemical sensing activity of rGO-Cr is monitored for paracetamol using modified glassy carbon electrode. Cyclic voltammetry measurements indicated that rGO-Cr substantially enhance the electrochemical response of paracetamol. The experimental factors are investigated and optimized.

KEYWORDS

anchored chromium complex, *cis-trans* switch, electrochemical detection of paracetamol, functionalization of GO/rGO, graphene oxide hybrid material, immobilized compounds, photoluminescence

1 | INTRODUCTION

The framework of graphene, the ‘amazing material’ of the scientific world has got ample attention due to its extraordinary optical,^[1] electronic^[2–4] and elastic properties.^[5] Moreover, graphene oxide (GO) stands for a new type of solution processable, non-stoichiometric macromolecule which can complex with many organic and inorganic systems with tunable properties. Graphene oxide has covalently decorated basal planes and edges with oxygen-containing functional groups, so that it contains a mixture of sp^2 and sp^3 hybridized

carbon atoms. The manipulation of the size, shape and relative fraction of the sp^2 hybridized domains of GO by reduction chemistry offers opportunities for tailoring its optoelectronic properties due to the heterogeneous chemical and electronic structures.^[6,7] Graphene oxide has a distinct band gap, well treated as a chemically tunable platform for optical applications by modern scientific community. Since it has many conductive electrons and holes, scientists have made many attempts to advance the dispersibility and compatibility of graphene framework through covalent and non-covalent functionalization.^[8–12]

Modern surface science is focusing on diazonium chemistry for the modification of materials, particularly carbon-based nanostructures. The successful modification of sp^2 carbon materials by diazonium chemistry introduced new strategies for the attachment of aryl layers to different organic and inorganic moieties, on account of the applications such as sensing,^[13] energy storage systems^[14] and molecular electronic junctions.^[15–17] Aryl diazonium compounds perform as precise coupling agents for polymers, biomacromolecules and nanoparticles which are extensively used for catalysis.^[18–22] Modification of materials by diazonium chemistry also provides a well-defined pathway to design and tune the optical properties for polymers fillers, polymer nanocomposites and polymer sensing layers. This also offers explicit routes to manipulate the nanorobots for cancer probes and drug delivery.^[19,23–34] Diazonium modification on graphene frame work appears promising since it results in significant increase of room temperature resistance and optical band gap of ~ 380 meV based on angle resolved photoemission electron microscopy measurements which leads graphene oxide as a potential material in optoelectronics.^[35–37] There are reports on functionalization of GO with highly conjugated aromatic molecules, polymers and ionic electrolytes.^[38–40] They are highly significant in heterogeneous catalysis,^[41–44] supercapacitors,^[45–47] adsorption and conversion of polluted gases.^[48–51]

In this work, we explored the possibility of covalent interaction through diazonium chemistry, to enhance the photoluminescence emission of graphene oxide. Reduced graphene oxide is functionalised by phenyl azo salicylaldehyde through silane coupling, based on known procedure.^[52] The coordination property of functionalised azo dye was studied by preparing its chromium (III) complex. The products isolated were characterised by Fourier transform infrared spectroscopy (FTIR), powder X-ray diffraction (PXRD), X-ray photoelectron spectroscopy (XPS), electron dispersive analysis of X-rays (EDAX), Raman spectroscopy, Scanning electron microscopy (SEM) and High resolution transmission electron microscopy (HRTEM). The absorption and excitation-dependent emission properties of PAS and rGO-TMSPA-PAS at room temperature were performed to understand the geometrical variations caused by an external stimulus and this can be used in developing a dynamic molecular devices. We also discuss the electrochemical detection of paracetamol by modified glassy carbon electrode with rGO anchored chromium complex. The comparative study of electrochemical performance of rGO/GCE and rGO-Cr/GCE presented an enhanced electrochemical response for rGO-Cr/GCE for paracetamol.

2 | EXPERIMENTAL SECTION

2.1 | Materials and methods

All chemicals used were of analytical grade. Graphite, potassium permanganate, sulphuric acid (36 M), HCl (5%), hydrogen peroxide (30%), trimethoxy silylpropanamine (TMSPA), aniline, salicylaldehyde, $CrCl_3 \cdot 6H_2O$ were purchased from Sigma Aldrich, Bangalore, India. Dipotassium hydrogen orthophosphate and potassium dihydrogen orthophosphate were obtained from Merck. Extra pure paracetamol was obtained from sd fine chemicals limited, India. All the reactions were carried out under an argon atmosphere with the use of standard Schlenk techniques. Toluene was purified and dried prior to the use. Dimethyl sulphoxide (DMSO) and ethanol were used without further purification.

2.2 | Synthesis of anchored chromium complex on reduced graphene oxide (rGO-Cr) through diazonium chemistry

2.2.1 | Synthesis of trimethoxysilyl propanamine functionalized reduced graphene oxide (rGO-TMSPA)

Graphene oxide (GO) was synthesized from graphite, by modified Hummers method^[53] and reduced graphene oxide was obtained by further thermal treatment of graphene oxide.

Trimethoxysilyl propanamine (TMSPA) functionalised reduced graphene oxide was prepared from reduced graphene oxide and TMSPA.^[52] Reduced graphene oxide (1.0 g) was sonicated in toluene for dispersion and refluxed with 3 mL of TMSPA under argon atmosphere for 24 hr. The product was washed with ethanol, filtered and dried at 50 °C.

2.2.2 | Synthesis of trimethoxysilyl propanamine phenyl azo salicylaldehyde functionalised reduced graphene oxide (rGO-TMSPA-PAS)

The 5-phenyl azo salicylaldehyde was prepared by the reported procedure.^[54] Aniline (2.26 ml) was mixed with 3 ml HCl (37%) in distilled water, diazotized at 5 °C. The diazotized aniline compound was coupled with salicylaldehyde in a mixture of sodium hydroxide and sodium carbonate at 5 °C at a pH of 7 to 9. Trimethoxy silyl propanamine functionalized reduced graphene oxide (500 mg) was dispersed in ethanol and refluxed with

5-phenyl azo salicylaldehyde (1.0 g) under argon atmosphere for 6 hr.

2.2.3 | Synthesis of anchored chromium complex on reduced graphene oxide (rGO-Cr)

Ethanollic dispersed solution of reduced graphene oxide 3-(trimethoxysilyl)-1-propanamine 5-phenyl azo salicylaldehyde (rGO-TMSPA-PAS) was mixed in an ethanollic solution of metal salt $\text{CrCl}_3 \cdot 6\text{H}_2\text{O}$ for 6 hr. The obtained immobilized complex was washed with ethanol to remove the unreacted reactants. The route of the synthesis of rGO anchored chromium complex is shown in Figure 1.

2.3 | Structural characterisation of anchored chromium complex on reduced graphene oxide

The IR spectra of rGO, rGO-TMSPA, rGO-TMSPA-PAS and rGO-Cr were recorded in Frontier IR spectrometer (Perkin Elmer) in the range $400\text{--}4000\text{ cm}^{-1}$ at room temperature. Powder X-ray Diffraction (PXRD) patterns of the samples were recorded with a Rigaku, Ultima IV using Ni-filtered $\text{Cu-K}\alpha$ X-ray source ($\lambda = 1.5406\text{ \AA}$). PXRD patterns were obtained in the 2θ range scanning from $10\text{--}90^\circ$ with a scan speed of 2° min^{-1} . The morphology of the functionalized rGO samples was characterized

by ultra High-Resolution Scanning Electron Microscopy (ULTRA 55 FESEM) and High Resolution Transmission Electron Microscopy (HRTEM JEOL JEM 2100). At room temperature, Micro-Raman spectra of the samples were recorded using HORIBA Jobin Yvon Lab RAM HR 800 equipped with a thermoelectrically cooled CCD detector. He-Ne laser of wavelength 632.81 nm with 20 mW of power was used as an excitation source. Chemical composition and states at the surface of rGO-Cr was done by X-ray Photoelectron Spectroscopy (XPS) (Thermo scientific K-alpha surface analysis). Shimadzu UV-2600 UV-Vis spectrophotometer was used to record UV-visible spectra using quartz cell with 1 cm path length. Photoluminescence studies were recorded in RF-5301 PC Shimadzu spectrofluorometer with slit width 5 nm and in the scan range of 220 nm to 770 nm . CHI660E electrochemical instrument was used for cyclic voltammetric studies.

3 | RESULTS AND DISCUSSION

The IR spectra of rGO, rGO-TMSPA, rGO-TMSPA-PAS, and rGO-Cr are shown in Figure 2. The appearance of the broad peak in pure rGO at 3393 cm^{-1} is attributed to the stretching vibration of carboxyl $-\text{OH}$. It is evidence for the occurrence of a number of hydroxyl groups. The other distinct peaks are 1710 cm^{-1} ($\text{C}=\text{O}$), 1149 cm^{-1} ($\text{C}-\text{OH}$) and 1031 cm^{-1} ($\text{C}-\text{O}$) represent the hydroxyl, carboxylic and epoxy groups.^[55–60] The FTIR spectrum

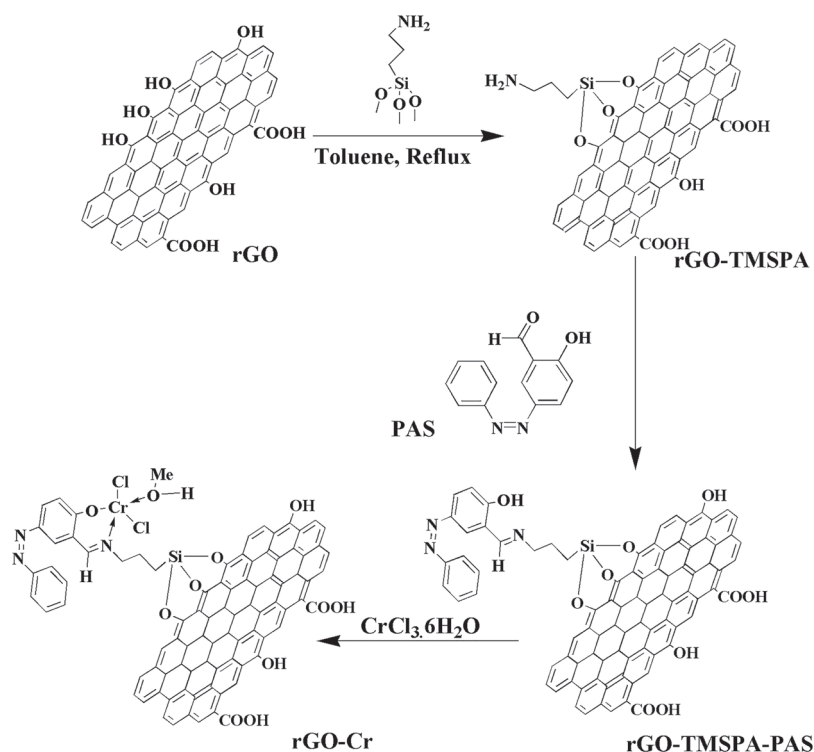


FIGURE 1 Schematic illustration of the synthesis of anchored chromium complex on reduced graphene oxide via silane and azo coupling

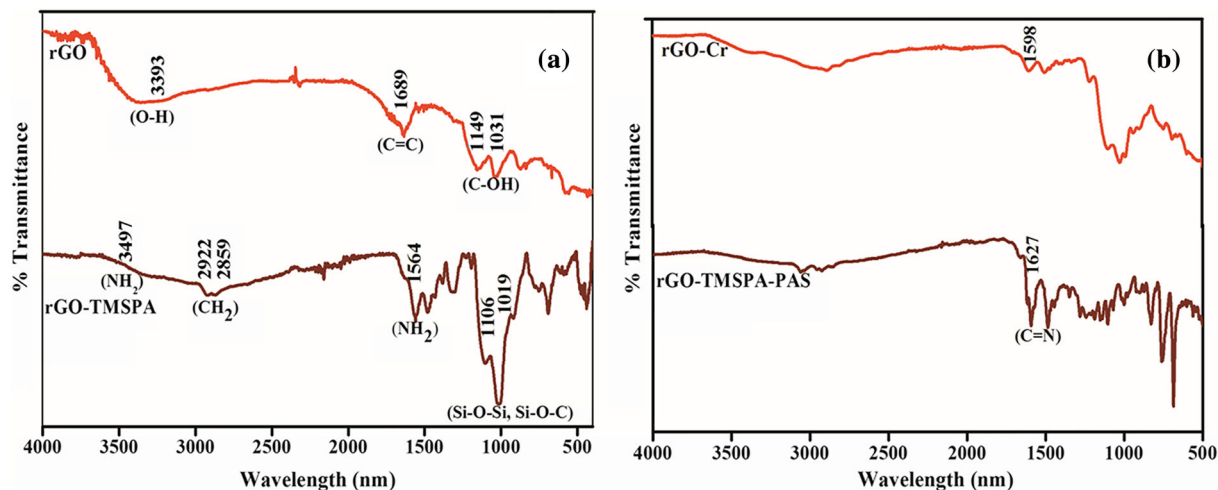


FIGURE 2 FTIR spectra of reduced graphene oxide and its functionalization by chromium complex through silane and azo coupling a. rGO and rGO-TMSPA b. rGO-TMSPA-PAS and rGO-Cr

of functionalized rGO shows several new peaks as compared to pure rGO. The doublet at 2922 cm^{-1} and 2859 cm^{-1} illustrate the asymmetric and symmetric alkyl chains of TMSPA. The vibrational bands of stretching and bending -NH_2 groups are at 3497 cm^{-1} and 1564 cm^{-1} respectively.^[32] The peaks at 1106 cm^{-1} and 1019 cm^{-1} correspond to the Si-O-Si and Si-O-C, confirms the silane coupling of rGO.^[53,61] The presence of these peaks reveals the anchoring of TMSPA onto reduced graphene oxide. The C=N frequency at 1627 cm^{-1} confirms the condensation reaction between the -NH_2 of rGO-TMSPA and -OH of 5-phenyl azo salicylaldehyde.^[55] The slight shift of the C=N frequency at 1598 cm^{-1} ($\Delta\nu$ is 29 cm^{-1}) confirmed the coordination of chromium (III) metal ion with azomethine nitrogen atom of functionalized rGO.^[34] The detailed IR spectrum of rGO, rGO-TMSPA, rGO-TMSPA-PAS and rGO-Cr are given in supporting information Figure S2.

Figure 3 displays the XRD pattern of rGO, rGO-TMSPA, rGO-TMSPA-PAS and rGO-Cr. The as prepared rGO shows a broad 2θ peak at 24.29° in (002) diffraction plane associated with reduced graphene oxide (rGO) of an interplanar distance 0.36 nm calculated by the Bragg's equation. This is due to the introduction of oxygenic functional groups and trapped water molecules between the graphite layers.^[41,62,63] During the anchoring of TMSPA, PAS and metal complex on the rGO surface, the diffraction peak of rGO do not disappear, indicating the structure of rGO is retained during the functionalization. However, it is clear from the XRD patterns that rGO-TMSPA, rGO-TMSPA-PAS, rGO-Cr are multilayered and illustrates a broad diffraction peak with an interplanar distance of 0.81 nm . This is attributed to increased layer to layer distance on further functionalisation of rGO.^[41,64,65]

In Raman spectra, graphene based materials display three major bands. The G band refers to the 1st order scattering of the E_{2g} and the D band is related to the out of plane modes of vibrations.^[38,39] The D-band intensity is directly related to the amount of disorder in the graphene sheets. 2D band, combination bands at 2723 cm^{-1} represents the graphite exfoliation and the activation of two phonons with identical momentum.^[66] Raman spectra of rGO and rGO-Cr are shown in Figure 4. The vibration

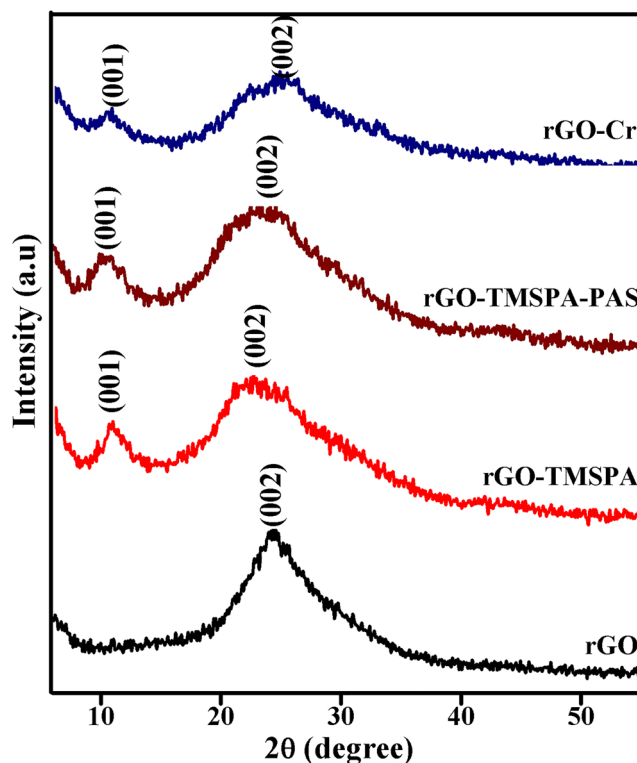


FIGURE 3 Powder XRD patterns of rGO, rGO-TMSPA, rGO-TMSPA-PAS, rGO-Cr

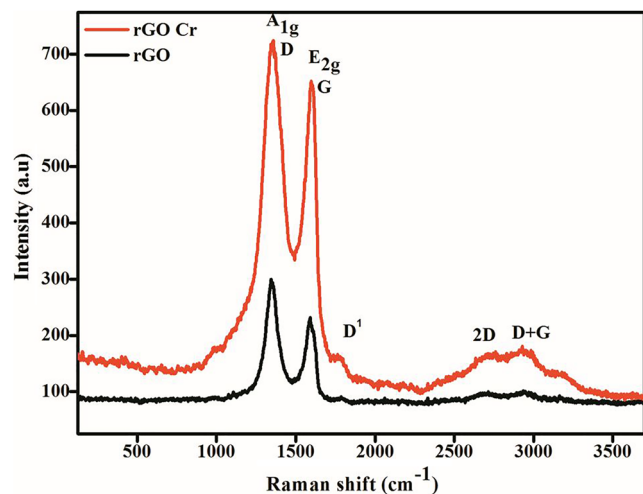


FIGURE 4 Measured Raman spectrum of reduced graphene oxide (rGO) and anchored chromium (III) complex on reduced graphene oxide (rGO-Cr)

of sp^2 hybridised carbon systems illustrate the G band at about 1595 cm^{-1} and D band at 1329 cm^{-1} corresponds to the distortions in the edge centred band structure of carbon framework of rGO.^[67] The intensity ratio I_D/I_G of rGO and rGO-Cr are 1.49 and 1.29 respectively. The broad D band compared to G band is owing to the structure disorders and defects in the graphene surface sheets.^[68] Here in after the functionalization of rGO, the G band shift to lower frequency region 1583 cm^{-1} , confirming the reduction and increasing number of layers in hybrid rGO.^[67] Decrease in I_D/I_G intensity ratio

indicates higher the degree of graphitization during the functionalisation in rGO-Cr.^[69,70]

Wide range X-ray photoelectron spectrum of the hybrid rGO-Cr complex on graphene oxide and their deconvoluted peaks are displayed in Figure 5 which reveals the presence of C1s, N1 s, O1s, Si2p, Cl2p, Cr2p_{1/2}, Cr2p_{3/2} at 284.6 eV, 401.2 eV, 532.1 eV, 102.6 eV, 195.9 eV, 587.1 eV and 577.3 eV respectively. The successful synthesis of rGO-covalently immobilized chromium (III) complex via diazonium chemistry was substantiated by the following: The highly resolved C1s spectrum was brought about four component peaks positioning at 284.4 eV, 286.4 eV, 285.3 eV, and 287.7 eV and are ascribed for C=C/C-C in GO aromatic rings, C=N of rGO-TMSPA-PAS, C-O in epoxy and alkoxy group of rGO and C=O in COOH of rGO respectively.^[71] The oxygen 1 s peak at 533.1 is revealed the C-OH in the functionalization of rGO.^[72,73] The distinctive resolution peak of N1 s obtained at 399.0 eV can be assigned to C=N-C of nitrogen.^[74–78]

To understand more about the morphology, microstructure and crystallinity rGO and rGO-Cr were examined by SEM and HRTEM. FESEM of rGO-Cr is shown in Figure 6. The loose agglomerates of tiny particles with a rough surface and irregular shapes are distributed in the extended sheet-like structures of rGO. For more clarity high resolution TEM images of rGO and rGO-Cr are presented in Figure 7. The white region refers to layered graphene sheet and the dark spots designate the anchored chromium complex through azo and silane coupling on rGO.

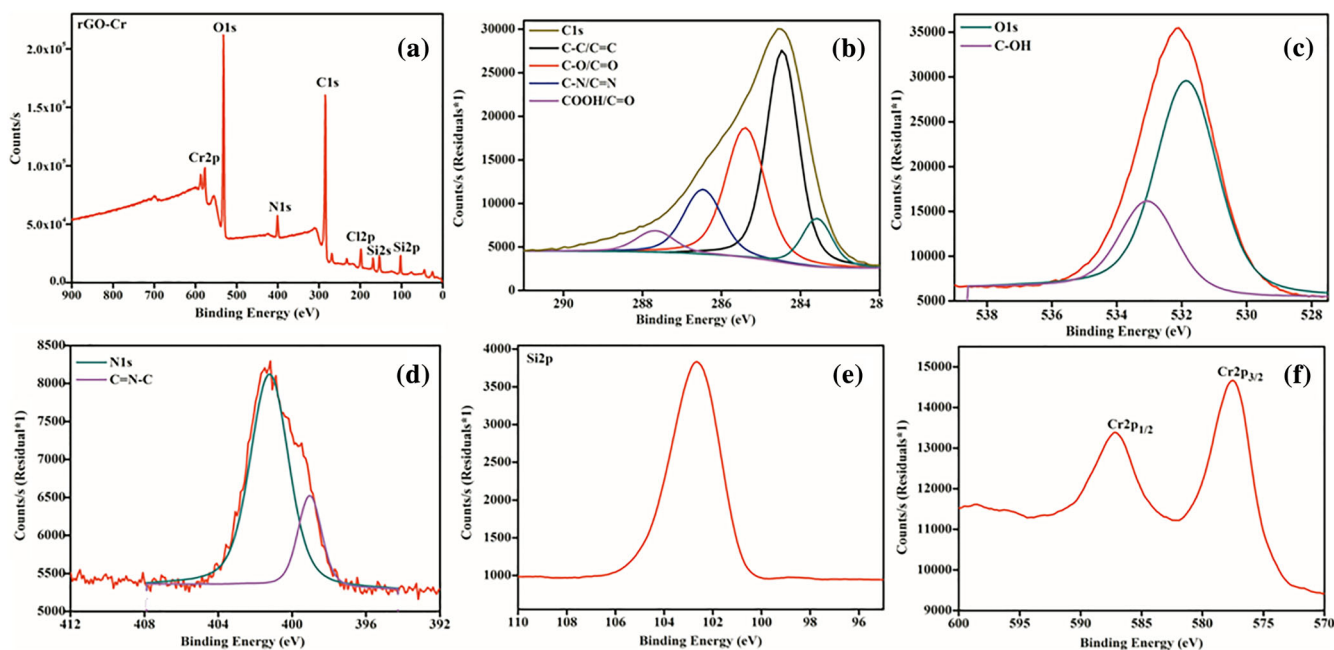


FIGURE 5 Wide-scan survey XPS spectrum of rGO-Cr (a) and Deconvoluted XPS peaks of C1s (b), O1s (c), N1 s (d), Si2p (e), Cr2p (f)

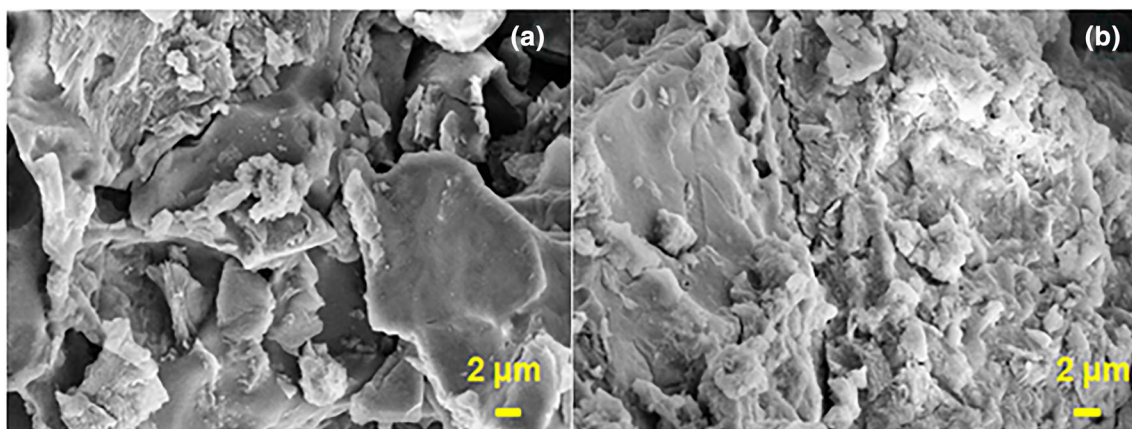


FIGURE 6 FESEM images of rGO-Cr

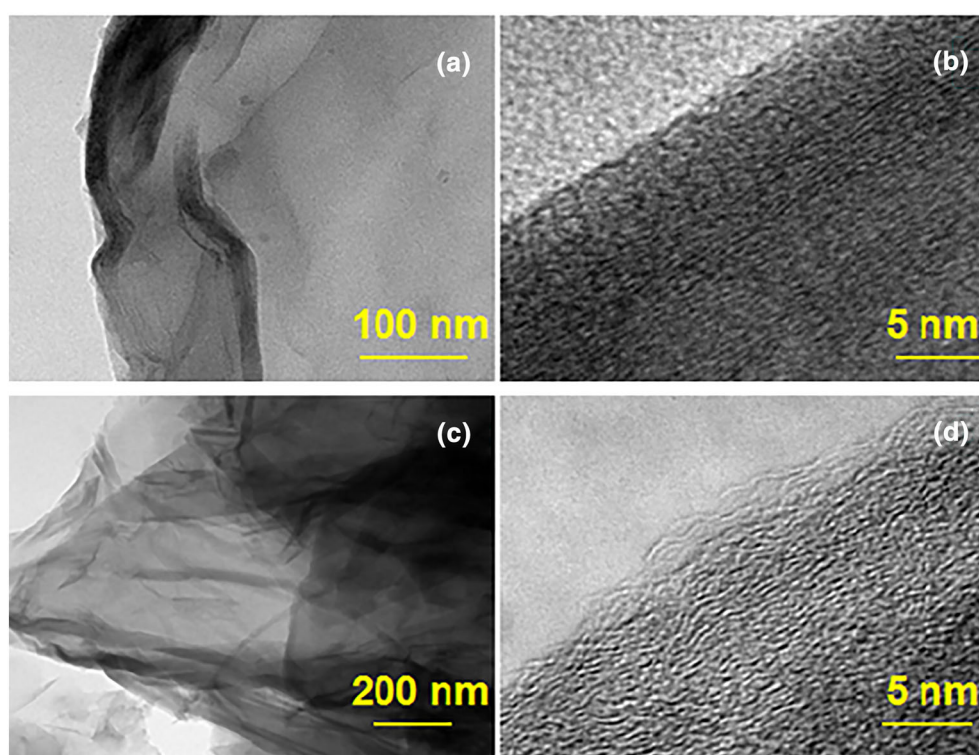


FIGURE 7 HRTEM images (a & b) rGO, (c & d) rGO-Cr

3.1 | Photoluminescence properties of rGO-TMSPA-PAS

The absorption and excitation-dependent emission properties of PAS and rGO-TMSPA-PAS at room temperature with the same concentration are shown in Figure 8. The literature reveals that rGO has a peak at 267 nm is due to the $\pi \rightarrow \pi^*$ transition band and the shoulder at ~ 320 nm corresponding to the $n \rightarrow \pi^*$ transition band of carbonyl group.^[55] The $\pi \rightarrow \pi^*$ transition band of PAS is at 274 nm. The other peaks are at 290 nm and 372 nm illustrating the $n \rightarrow \pi^*$ transition of the N=N

and C=O absorptions respectively. The peak at 455 nm in the PAS spectrum is associated with the cis to trans isomeric switching of the PAS molecule.^[79] The dissolved form of PAS molecule is known to switch from the cis to trans at room temperature, in presence of an electric field or under UV irradiation.^[80] Trans isomer of azo benzene is more stable than cis isomer due to the less exothermic heat of combustion.^[81] It is also predominant in dark at room temperature and the photoexcited state is at ~ 23 kcal mol⁻¹.^[82] The trans PAS isomerises to cis PAS with a wavelength of 372 nm and gets back to trans at 455 nm when it absorbs a photon and it is shown in

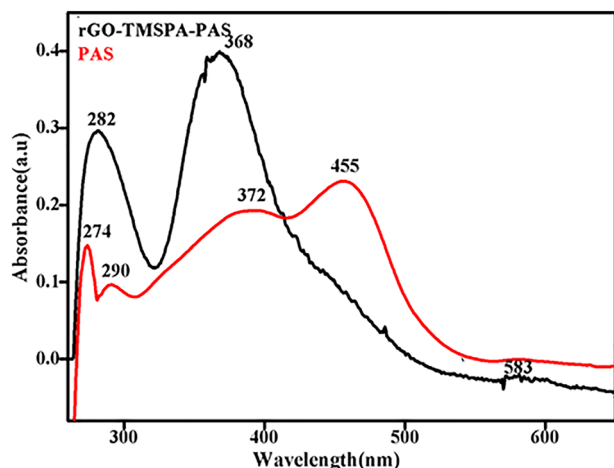


FIGURE 8 Absorption properties of PAS and rGO-TMSPA-PAS showing the excimer at 583 for rGO-TMSPA-PAS

Figure 9. Azobenzenes easily undergo isomerisation. In the wavelength between 320–350 nm, trans isomer isomerises to cis isomer by irradiation ($S_1 \leftarrow S_0$ and $S_2 \leftarrow S_0$ excitations). It reverts back to trans isomer when it absorbs light between 400–450 nm by exciting into the S_1 or S_2 state.^[83] This photoinduced isomerisation of the azobenzenes leads to a remarkable change in their physical properties which make them as potential molecular switches. The UV spectrum of GO-TMSPA-PAS in DMSO gives three peaks at 282 nm, 368 nm and a less intense peak at 455 nm. The peak at 282 nm indicates the absorption of rGO in the functionalized PAS because of the π electron interaction of rGO and TMSPA-PAS. The peaks at 368 and 455 nm are designated as the $n \rightarrow \pi^*$ transitions of the GO-TMSPA functionalized azo dye.^[84] The wavelengths and intensity shifts in the absorption bands of PAS and covalently grafted rGO-TMSPA-PAS proposing the electronic communication and π - π interactions between the electron donor PAS and electron acceptor rGO-TMSPA. The excimer peak at 583 nm is attributed to an electronically excited dimer of the rGO-TMSPA-PAS. The UV spectral values of rGO, rGO-TMSPA, PAS, rGO-TMSPA-PAS are represented in Table 1.

TABLE 1 UV-Visible transitions of rGO, rGO-TMSPA, PAS and rGO-TMSPA-PAS

Wavelength	$\pi \rightarrow \pi^*$ (nm)	$n \rightarrow \pi^*$ (nm)
rGO	267	320 ^[85]
rGO-TMSPA	249	297 ^[55]
PAS	274	290, 372, 455
rGO-TMSPA-PAS	282	368, 455

The cis-trans switch of PAS initiates the change in the photoluminescence performances of pure and hybrid PAS. To understand the photoluminescence properties of the same, excitation dependent photoluminescence measurements were performed at 282 nm, 368 nm, 372 nm and 455 nm as shown in Figure 10. It is seen that, as the excitation wavelength of both PAS and rGO-TMSPA-PAS increases, the emission peaks also move towards from green to red in visible light with different intensities. GO exhibits the emission bands at 438 nm and 500 nm at the excitation wavelength of 360 nm.^[48] The excitation dependent photoluminescence spectrum of PAS and rGO-TMSPA-PAS at 455 nm shows broad bands with higher intensity for rGO-TMSPA-PAS compared to PAS. The broad emission peak in the range of 500 nm to 850 nm is due to the $\pi \rightarrow \pi^*$ gap created by the structure distortions which in turn result in the optical transitions among the localised states.^[48] Photoluminescence spectra also substantiate that the emission emerges from four different regions, viz., green, yellow, orange and red. This means that the fluorescence colour of both PAS and rGO-TMSPA-PAS could be turned simply by changing the excitation wavelength. The emission intensity of PAS at excitation wavelength 455 nm is decreased by ~75% compared to 372 nm. It is inferred that this change in photoluminescence is due to the fact that the major part of the energy at 455 nm excitation is used for isomeric switching. Thus the resultant emission spectrum is due to the residual energy present in the excitation radiation. Such an inference is supported by previous reports

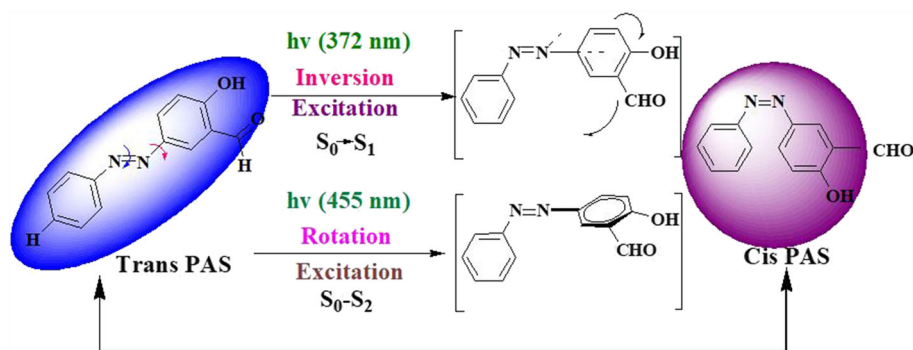


FIGURE 9 Cis-Trans switch of phenyl azo salicylaldehyde at 372 and 455 nm

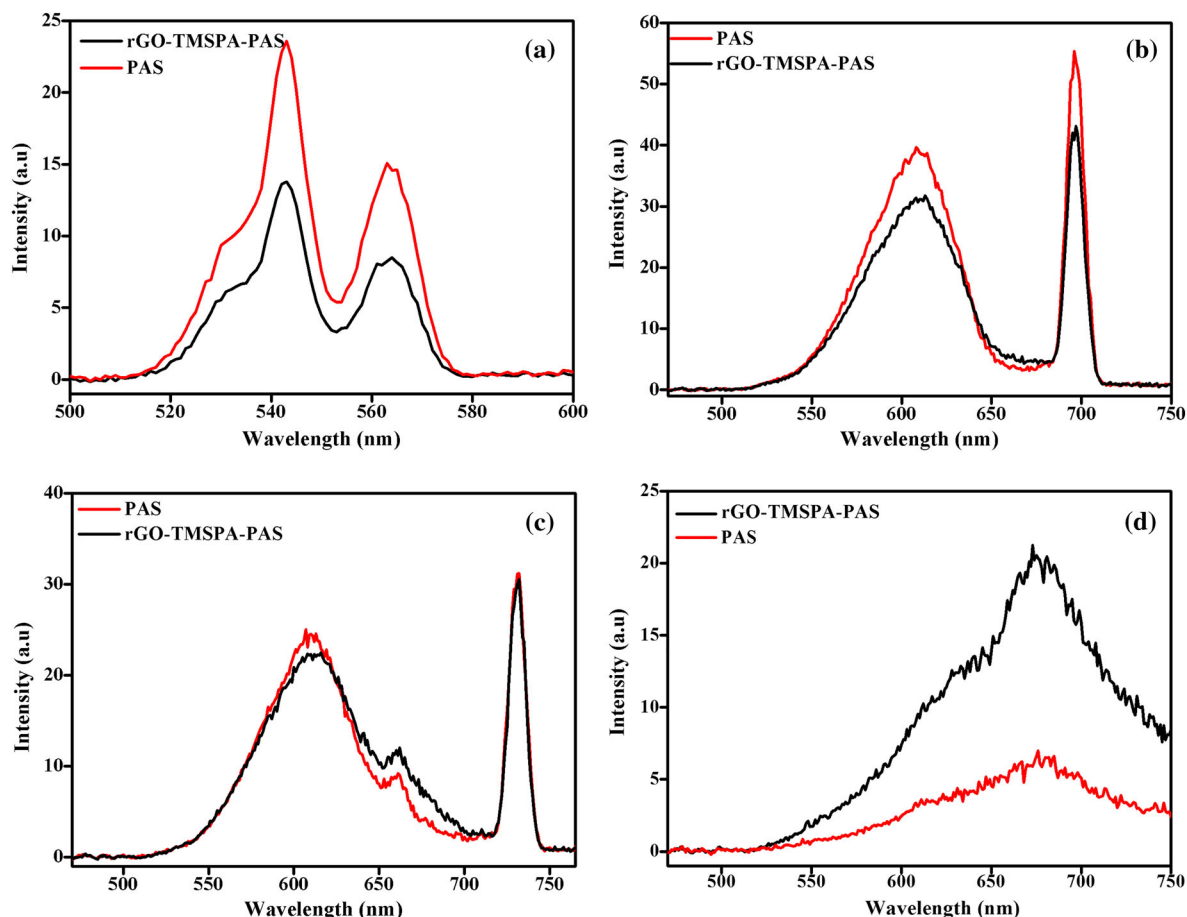


FIGURE 10 Photoluminescence spectra of PAS and GO-TMSPA-PAS in dimethyl sulphoxide at an excitation wavelength a) 282 nm b) 368 nm c) 372 nm and d) 455 nm

studying cis- trans switch in PAS derivatives.^[42,80,86] The special features of the excitation dependent photoluminescence spectra signify the capturing of electrons of the rGO-TMSPA from PAS.^[87] This enhances the electron hole pairs and hence, the photoluminescence quenching. These studies can lead to a better route for the solution processable optoelectronics material.

3.2 | Electrochemical studies of anchored chromium complex on reduced graphene oxide (rGO-Cr)

Cyclic voltammetry and differential pulse voltammetry (DPV) were used to resolve the electrochemical sensing properties of rGO anchored chromium complex for paracetamol. The electrochemical experiments were carried out in 0.1 M phosphate buffer solution (PBS), pH 7 in a three electrode system using the bare and modified GCE as the working electrode, platinum wire as the counter electrode and Ag/AgCl electrode as the reference electrode to examine the electrochemical activity of the rGO anchored chromium complex. For cyclic voltammetry

measurements, the sensors were immersed in 30 ml of 0.1 M PBS containing 0.1 mg ml⁻¹ applying the potential in the range of -0.2 V to 0.6 V. Differential pulse scanning voltammetry was carried out in -0.4 to 0.8 V with an increment of 0.004 V, an amplitude of 0.05 V along with a pulse width of 0.05 s using 0.1 M phosphate buffer as the background electrolyte. The GCE surface was modified manually by drop casting the synthesised materials on the working area. A comparative study using a bare and modified electrode (GCE/rGO, GCE/rGO-Cr) in the presence of 1 mM K₄Fe(CN)₆ in 0.1 M KCl solution was conducted. Electrochemical studies were further carried out for the detection of paracetamol in 0.1 M phosphate buffer solution (pH -7).

The electrochemical behavior of paracetamol at rGO-Cr modified GCE (rGO-Cr/GCE) was investigated by cyclic voltammetry. As shown in Figure 11 (a), the rGO-Cr modified/GCE shows the highest peak current response in comparison to bare and other modified electrodes in the presence of a redox species 1 mM K₄Fe(CN)₆ in 0.1 M KCl at 100 mVs⁻¹. Figure 11 (b) represents an increased electrocatalytic current response of bare GCE, rGO/GCE, rGO-Cr/GCE individually in the presence of

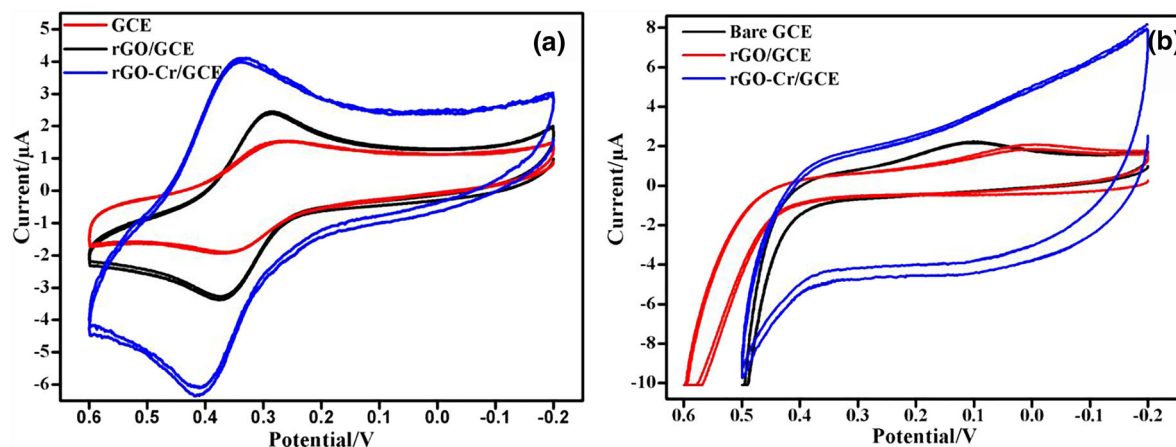


FIGURE 11 (a) Cyclic voltammogram CV) of the bare GCE, rGO/GCE and rGO-Cr/GCE in the presence of 1 mM ferro/ferricyanide in 0.1 M KCl at 100 mVs⁻¹. (b) Development of the Electrocatalytic behaviour of rGO-Cr/GCE compared to bare GCE, rGO/GCE and rGO-Cr/GCE in the presence of 0.1 mg ml⁻¹ (0.6 mM) paracetamol in PBS (pH = 7)

0.1 mg ml⁻¹ (0.6 mM) paracetamol (pH = 7) at the scan rate of 100 mVs⁻¹. The rGO-Cr/GCE gives the maximum current response and also a positive potential shift compared with the bare GCE. The potential shift is due to the increased electron transfer mechanism between the modified electron surface and the oxidizable species (paracetamol). It is evident that the rGO-Cr/GCE could be an effective electrocatalyst for the redox reaction of paracetamol and it is facilitated by the electron transfer between the electrode and analyte.

3.2.1 | Optimization of scan rate and concentration of analyte

The effect of scan rate on the electrochemical redox process of paracetamol at rGO-Cr/GCE was studied in

0.1 M buffer. Figure 12 (a) shows a series of cyclic voltammograms for rGO-Cr/GCE with the scan rate range from 50 mVs⁻¹ to 225 mVs⁻¹. The scan rate effect also gives information about the mechanism which involved in electrochemical redox process of paracetamol. The redox peak current at the modified electrode was linearly increased with increasing in the scan rate and is shown in Figure 12 (b).

Differential pulse voltammetry (DPV) technique was performed to understand the association between peak current and concentration of paracetamol. Differential pulse voltammetry of rGO-Cr/GCE in 0.1 M phosphate buffer in different concentrations of paracetamol is shown in the Figure 13, which signifies a linear relationship between the peak current and concentration of the analyte. The peak obtained at 0.4 V is due to the oxidation of paracetamol to N-(4-oxo-cyclohexa-2,

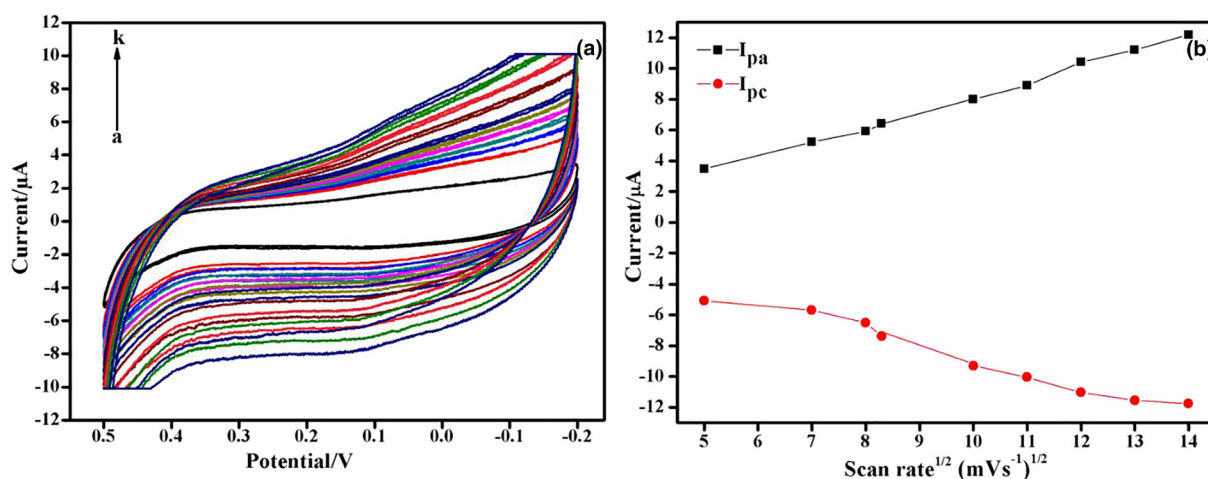


FIGURE 12 (a) Cyclic voltammograms of the rGO-Cr/GCE in 0.1 M PBS containing 0.1 mg ml⁻¹ paracetamol at different scan rates 50,60,70,80,90,100,125,150,175,200 mVs⁻¹, respectively. (b) Variations of anodic peak current (I_{pa}) and cathodic peak current (I_{pc}) with the square root of the scan rate

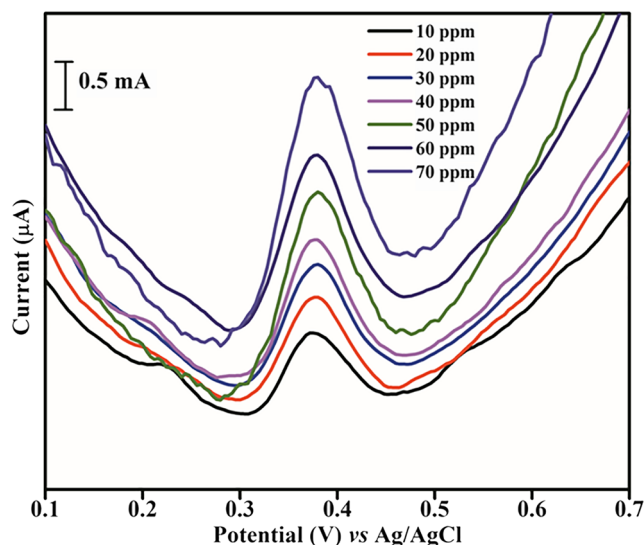


FIGURE 13 Differential pulse voltammetry of rGO-Cr/GCE in 0.1 M phosphate buffer with different concentrations of paracetamol like 10 ppm, 20 ppm, 30 ppm, 40 ppm, 50 ppm, 60 ppm and 70 ppm

5 dienyldiene)-acetamide. The linear relationship of peak current with concentration of analyte will be helpful for the quantitative electrochemical determination of rGO-Cr for the detection of paracetamol.

4 | CONCLUSION

In summary, trimethoxysilyl propanamine phenyl azo salicylaldehyde functionalized rGO (rGO-TMSPA-PAS) and its mononuclear chromium complex are synthesised through diazonium chemistry. The spectroscopic and morphological studies supported the successful syntheses of rGO, rGO-TMSPA, rGO-TMSPA-PAS and rGO-Cr. Powder XRD studies and Raman spectra showed the distortions of the framework of graphene surface due to the functionalization. The FESEM and HRTEM images revealed that sheet structure of rGO is retained in a large extent during the multistep synthesis. Elemental analysis like XPS is well supported the functionalization of rGO. Amazing emission properties in the range of 542 nm to 732 nm were observed for functionalized azo dye on graphene oxide through silane coupling (rGO-TMSPA-PAS) and free azo dye (PAS) with an excitation dependent photoluminescence study at room temperature. Photoluminescence studies experience a red shift, with a decrease in intensity when the excitation wavelength increases. These results demonstrate that both silane functionalized graphene oxide and azo dye enable an electronic interaction due to the recombination of sp^2 and sp^3 states and electron-hole pairs which have extensive importance in developing optoelectronic devices. The

rGO-Cr complex showed an enhanced electrocatalytic activity which was utilized for the fabrication of the sensitive electrode for the quantitative detection of paracetamol.

ACKNOWLEDGMENTS

The work was financially supported by Centre for Research, CHRIST (Deemed to be University), Bengaluru, India. SPB is thankful to Prem Prabhakar, Hannam University Daejeon, South Korea and Sadasivan Shaji, Autonomous University of Nuevo Leon, Mexico.

ORCID

Sreekanth Anandaram  <https://orcid.org/0000-0002-2942-8487>

Sreeja P B  <https://orcid.org/0000-0002-2106-7867>

REFERENCES

- [1] K. P. Loh, Q. Bao, G. Eda, M. Chhowalla, *Nat. Chem.* **2010**, 2, 1015.
- [2] K. S. Novoselov, A. K. Geim, S. V. Morozov, D. Jiang, Y. Zhang, S. V. Dubonos, I. V. Grigorieva, A. A. Firsov, *Science* **2012**, 306, 666.
- [3] K. I. Bolotin, K. J. Sikes, Z. Jiang, M. Klima, G. Fudenberg, J. Hone, P. Kim, H. L. Stormer, *Solid State Commun.* **2008**, 146, 351.
- [4] Y. Zhang, Y. W. Tan, H. L. Stormer, P. Kim, *Nature* **2005**, 438, 201.
- [5] C. Gómez-Navarro, M. Burghard, K. Kern, *Nano Lett.* **2008**, 8, 2045.
- [6] C. Gómez-Navarro, R. T. Weitz, A. M. Bittner, M. Scolari, A. Mews, M. Burghard, K. Kern, *Nano Lett.* **2007**, 7, 3499.
- [7] Z. Z. Zhang, K. Chang, *Phys. Rev. B* **2008**, 77, 1.
- [8] K. C. Kemp, V. Georgakilas, M. Otyepka, A. B. Bourlinos, V. Chandra, N. Kim, K. C. Kemp, P. Hobza, R. Zboril, K. S. Kim, *Chem. Rev.* **2012**, 112, 6156.
- [9] A. Ghosh, K. V. Rao, S. J. George, C. N. R. Rao, *Chem. – Eur. J.* **2010**, 16, 2700.
- [10] M. Liu, R. Zhang, W. Chen, *Chem. Rev.* **2014**, 114, 5117.
- [11] X. Gong, G. Liu, Y. Li, D. Y. W. Yu, W. Y. Teoh, *Chem. Mater.* **2016**, 28, 8082.
- [12] S. Obata, K. Saiki, T. Taniguchi, T. Ihara, *J. Phys. Soc. Jpn.* **2015**, 121012, 1.
- [13] C. Cao, Y. Zhang, C. Jiang, M. Qi, G. Liu, *ACS Appl. Mater. Interfaces* **2017**, 9, 5031.
- [14] B. D. Assresahegn, T. Brousse, D. Bélanger, *Carbon* **2015**, 92, 362.
- [15] Z. Lu, S. Yang, Q. Yang, S. Luo, C. Liu, Y. Tang, *Microchim. Acta* **2013**, 180, 555.
- [16] M. M. Bernal, A. D. Pierro, C. Novara, F. Giorgis, B. Mortazavi, G. Saracco, A. Fina, *Adv. Funct. Mater.* **2018**, 28, 1.
- [17] X. Zhang, L. Hou, *Nat. Commun.* **2016**, 7, 1.

- [18] A. A. Mohamed, Z. Salmi, S. A. Dahoumane, A. Mekki, B. Carbonnier, M. M. Chehimi, *Adv. Colloid Interface Sci.* **2015**, 225, 16.
- [19] M. P. Sandomierski, B. Strzemiescka, M. M. Chehimi, A. Voelkel, *Langmuir* **2016**, 32, 11646.
- [20] J. O. Zoppe, N. C. Ataman, P. Mocny, J. Wang, J. Moraes, H. Klok, *Chem. Rev.* **2017**, 117, 1105.
- [21] N. Oger, F. A. Felpin, *ChemCatChem* **2016**, 8, 1998.
- [22] S. Mahouche-Chergui, S. Gam-Derouich, C. Mangeney, M. M. Chehimi, *Chem. Soc. Rev.* **2011**, 40, 4143.
- [23] C. M. Homenick, G. Lawson, A. Adronov, *Polym. Rev.* **2007**, 47, 265.
- [24] M. B. Lerner, J. D'Souza, T. Pazina, J. Dailey, B. R. Goldsmith, M. K. Robinson, A. T. C. Johnson, *ACS Nano* **2012**, 6, 5143.
- [25] A. Gupta, S. K. Saha, *Nanoscale* **2012**, 4, 6562.
- [26] S. Mondal, A. Gupta, B. Kumar, S. K. Saha, *Opt. Mater.* **2017**, 73, 555.
- [27] S. K. Vashist, D. Zheng, G. Pastorin, K. Al-Rubeaan, J. H. T. Luong, F. S. Sheu, *Carbon* **2011**, 49, 4077.
- [28] G. Xu, J. Wang, G. Si, M. Wang, H. Cheng, B. Chen, S. Zhou, *Dyes Pigment.* **2017**, 141, 470.
- [29] J. J. Ding, H. X. Chen, D. Q. Feng, H. W. Fu, *IOP Conf. Ser. Mater. Sci. Eng.* **2018**, 292, 1.
- [30] S. Biswas, C. S. Tiwary, S. Vinod, A. K. Kole, U. Chatterjee, P. Kumbhakar, P. M. Ajayan, *J. Phys. Chem. C* **2017**, 121, 8060.
- [31] R. Liu, J. Hu, S. Zhu, J. Lu, H. Zhu, *ACS Appl. Mater. Interfaces* **2017**, 9, 33029.
- [32] P. Guarracino, T. Gatti, N. Canever, M. Abdu-Aguye, M. A. Loi, E. Menna, L. Franco, *Phys. Chem. Chem. Phys.* **2017**, 19, 27716.
- [33] R. Devi, G. Prabhavathi, R. Yamuna, S. Ramakrishnan, N. K. Kothurkar, *J. Chem. Sci.* **2014**, 126, 75.
- [34] S. Jeon, S. Kwak, D. Yim, J. Ju, J. Kim, *J. Am. Chem. Soc.* **2014**, 31, 10842.
- [35] G. L. C. Paulus, Q. H. Wang, M. S. Strano, *Acc. Chem. Res.* **2013**, 46, 160.
- [36] G. Eda, Y.-Y. Lin, C. Mattevi, H. Yamaguchi, H. Chen, I. Chen, C. Chen, M. Chhowalla, *B. Adv. Mater.* **2009**, 22, 1.
- [37] S. Niyogi, E. Bekyarova, M. E. Itkis, H. Zhang, K. Shepperd, J. Hicks, M. Sprinkle, C. Berger, C. N. Lau, W. A. Deheer, E. H. Conrad, R. C. Haddon, *Nano Lett.* **2010**, 10, 4061.
- [38] J. R. Herance, M. Alvaro, *Chem. – Eur. J.* **2017**, 23, 15244.
- [39] B. I. Kharisov, O. V. Kharissova, A. V. Dimas, G. D. L. Fuente, Y. P. Méndez, *J. Coord. Chem.* **2016**, 69, 1125.
- [40] R. Yadav, A. Subhash, N. Chemmenchery, B. Kandasubramanian, *Ind. Eng. Chem. Res.* **2018**, 57, 9333.
- [41] S. Rayati, E. Khodaei, S. Shokoohi, M. Jafarian, B. Elmi, A. Wojtczak, *Inorganica Chim. Acta* **2017**, 466, 520.
- [42] S. Omid, A. Kakanejadifard, F. Azarbani, *J. Mol. Liq.* **2017**, 242, 812.
- [43] Z. Li, S. Wu, H. Ding, D. Zheng, J. Hu, X. Wang, Q. Huo, J. Guan, Q. Kan, *New J. Chem.* **2013**, 37, 1561.
- [44] Z. Li, S. Wu, H. Ding, H. Lu, J. Liu, Q. Huo, J. Guan, Q. Kan, *RSC Adv.* **2013**, 4, 9990.
- [45] K. Vijayasankar, R. Kalaiselvan, *Electrochim. Acta* **2016**, 20, 469.
- [46] H. Wang, L. Ma, M. Gan, T. Zhou, X. Sun, W. Dai, H. Wang, S. Wang, *Composites Part B Eng.* **2016**, 92, 405.
- [47] J. Yang, E. Zhang, X. Li, Y. Yu, J. Qu, Z. Yu, *ACS Appl. Mater. Interfaces* **2015**, 8, 2297.
- [48] D. Dinda, A. Gupta, B. K. Shaw, S. Sadhu, S. K. Saha, *ACS Appl. Mater. Interfaces* **2014**, 6, 10722.
- [49] P. Bhanja, S. K. Das, A. K. Patra, A. Bhaumik, *RSC Adv.* **2016**, 6, 72055.
- [50] S. Kumar, P. Kumar, A. Deb, D. Maiti, S. L. Jain, *Carbon* **2016**, 100, 632.
- [51] P. Kumar, B. Sain, S. L. Jain, *J. Mater. Chem. A* **2014**, 2, 11246.
- [52] S. Rana, S. B. Jonnalagadda, *Catal. Commun.* **2017**, 92, 31.
- [53] S. Verma, M. Aila, S. Kaul, S. L. Jain, *RSC Adv.* **2014**, 4, 30598.
- [54] M. S. Refat, I. M. El-deen, H. K. Ibrahim, S. El-ghool, *Spectrochim. Acta a* **2006**, 65, 1208.
- [55] S. Kumari, A. Shekhar, D. D. Pathak, *RSC Adv.* **2016**, 6, 15340.
- [56] H. P. Mungse, S. Verma, N. Kumar, B. Sain, O. P. Khatri, *J. Mater. Chem.* **2012**, 22, 5427.
- [57] M. S. Nejad, S. Behzadi, H. Sheibani, *Appl. Organometal Chem.* **2019**, 1, e4804.
- [58] H. Su, Z. Li, Q. Huo, J. Guan, Q. Kan, *RSC Adv.* **2014**, 4, 9990.
- [59] K. Karami, A. Ramezanpour, M. Zakariazadeh, C. Silvestru, *Appl. Organometal Chem.* **2019**, 1, e4907.
- [60] M. Rohaniyan, A. Davoodnia, S. A. Beyramabdi, *Appl. Organometal Chem.* **2019**, 1, e4881.
- [61] A. M. Santos, F. E. Kühn, W. M. Xue, E. Herdtweck, *J. Chem. Soc. Dalton Trans.* **2000**, 1, 3570.
- [62] A. Jabbar, G. Yasin, W. Q. Khan, M. Y. Anwar, R. M. Korai, M. N. Nizam, G. Muhyodin, *RSC Adv.* **2017**, 7, 31100.
- [63] S. K. Mishra, S. N. Tripathi, V. Choudhary, B. D. Gupta, *Sens. Actuators B Chem.* **2014**, 199, 190.
- [64] S. Park, K. S. Lee, G. Bozoklu, W. Cai, S. B. T. Nguyen, R. S. Ruoff, *ACS Nano* **2008**, 2, 572.
- [65] A. Yang, J. Li, C. Zhang, W. Zhang, N. Ma, *Appl. Surf. Sci.* **2015**, 346, 443.
- [66] Q. A. Khan, A. Shaur, T. A. Khan, Y. F. Joya, M. S. Awan, Q. A. Khan, A. Shaur, T. A. Khan, Y. F. Joya, M. S. Awan, *Cogent Chem.* **2017**, 3.
- [67] M. A. Jhonsi, C. Nithya, A. Kathiravan, *Chem. Phys.* **2014**, 16, 20878.
- [68] T. S. Sreeprasad, S. M. Maliyekkal, K. P. Lisha, T. Pradeep, *J. Hazard. Mater.* **2011**, 186, 921.
- [69] S. P. Jose, C. S. Tiwary, S. Kosolwattana, P. Raghavan, L. D. Machado, C. Gautam, T. Prasankumar, J. Joyner, S. Ozden, D. S. Galvao, P. M. Ajayan, *RSC Adv.* **2016**, 6, 93384.
- [70] L. Y. Ma, J. Chen, W. Chen, D. Y. Lee, *Jim, Nano Energy* **2014**, 144.
- [71] L. X. Xue, T. T. Meng, Y. Zhao, L. H. Gao, K. Z. Wang, *Electrochim. Acta* **2015**, 172, 77.
- [72] Y. J. Oh, J. J. Yoo, Y. I. Kim, J. K. Yoon, H. N. Yoon, J. H. Kim, S. B. Park, *Electrochim. Acta* **2014**, 116, 118.
- [73] S. Wenmackers, P. Christiaens, W. Deferme, M. Daenen, K. Haenen, M. Nesládek, P. Wagner, V. Vermeeren, L. Michiels, M. vandeVen, M. Ameloot, J. Wouters, L. Naelaerts, Z. Mekhalif, *Mater. Sci. Forum* **2005**, 267, 492.

- [74] N. Hellgren, R. T. Haasch, S. Schmidt, L. Hultman, I. Petrov, *Carbon* **2016**, 108, 242.
- [75] I. Bertóti, M. Mohai, K. László, *Carbon* **2015**, 84, 185.
- [76] Y. Yamada, J. Kim, S. Matsuo, S. Sato, *Carbon* **2014**, 70, 59.
- [77] A. Mohtasebi, T. Chowdhury, L. H. H. Hsu, M. C. Biesinger, P. Kruse, *J. Phys. Chem. C* **2016**, 120, 29248.
- [78] Y. Xu, Z. Li, F. Zhang, X. Zhuang, Z. Zeng, J. Wei, *RSC Adv.* **2016**, 6, 30048.
- [79] K. G. Yager, C. J. Barrett, *J. Photochem. Photobiol. Chem.* **2006**, 182, 250.
- [80] E. Merino, M. Ribagorda, *Beilstein J. Org. Chem.* **2012**, 8, 1071.
- [81] H. Rau, *Angew. Chem Int. Ed.* **1973**, 12, 224.
- [82] E. V. Brown, G. R. Granneman, *J. Am. Chem. Soc.* **1975**, 97, 621.
- [83] Q. I. N. Chuan-guang, L. U. Cai-xia, O. Gao-wei, Q. I. N. Ke, Z. Feng, S. H. I. Hai-tong, W. Xiao-hui, *Chin. J. Anal. Chem.* **2015**, 43, 433.
- [84] A. Misra, M. Shahid, *J. Phys. Chem. C* **2010**, 114, 16726.
- [85] L. H. Urner, B. N. S. Thota, O. Nachtigall, S. Warnke, G. Von Helden, R. Haag, K. Pagel, *Chem. Commun.* **2015**, 51, 8801.
- [86] M. Aleksandrak, W. Kukulka, E. Mijowska, *Appl. Surf. Sci.* **2017**, 398, 56.
- [87] S. P. Kumar, K. Giribabu, R. Manigandan, S. Munusamy, S. Muthamizh, A. Padmanaban, T. Dhanasekaran, R. Suresh, V. Narayanan, *Electrochimica Acta* **2016**, 194, 116.

SUPPORTING INFORMATION

Additional supporting information may be found online in the Supporting Information section at the end of the article.

How to cite this article: Jose J, Rajamani AR, Anandaram S, Jose SP, Peter SC, P B S. Photophysical and Electrochemical Studies of Anchored Chromium (III) Complex on Reduced Graphene Oxide via Diazonium Chemistry. *Appl Organometal Chem.* 2019;e5063. <https://doi.org/10.1002/aoc.5063>